The Lateral Surface Drag Coefficient of Cylindrical Spacecraft in a Rarefied Finite Temperature Atmosphere

F. A. Herrero*
NASA Goddard Space Flight Center, Greenbelt, Maryland

The free-molecule flow drag coefficient is obtained for a cylindrical spacecraft flying parallel to its principal axis. The effect of thermal motion on the lateral surface is included explicitly in terms of the average impact angle of the incident gas momentum vector. The total drag force is given in terms of the drag coefficient of the front face or nose cone, the length and radius of the cylinder, and a lateral surface coefficient which arises from molecular impacts at near-grazing incidence. Existing kinetic theory results are used to describe self shadowing and to obtain an expression for the lateral surface coefficient in terms of the average impact angle of the incident momentum vector and the fractional momentum transfer along the line of impact. The latter can be estimated from extrapolation of laboratory measurements, and the average impact angle is derived from kinetic theory. The expression obtained for the total drag coefficient is used to estimate the lateral surface coefficient using existing flight data for one cylindrical spacecraft. The result compares favorably with the number obtained using the laboratory data. It is found that for a length-to-diameter ratio of about 5, the lateral surface contribution to the drag coefficient is comparable to that of the front face.

Introduction

THIS paper is concerned with the drag coefficient of a cylindrical spacecraft flying parallel to its principal axis, i.e., at zero angle of attack. The total drag force is decomposed into the sum of the forces on the front face and lateral surface. The force on the front face is computed in a manner similar to previous methods ignoring the effect of thermal motion in the atmosphere, and the lateral surface drag is computed taking into account the thermal motion explicitly. The resulting formula for the drag coefficient is then evaluated using laboratory data, and the value obtained is compared with existing flight data.

We consider only right circular cylinder forms moving in a rarefied atmosphere such that λ_0, the mean free path in the freestream, is much larger than the representative dimension D (e.g., width) of the spacecraft; that is, the Knudsen number $K=D/\lambda_0 \gg 1$. This condition guarantees that no molecules reemitted from the surface collide with molecules in the gas near the spacecraft.[1] It is satisfied roughly in the Earth's atmosphere at altitudes above about 150 km for typical spacecraft dimensions of about 1 m. In such a case K is between 30 and 40 in the freestream. However, if significant energy accommodation takes place[1] at the spacecraft surface, the reflected molecules move with a velocity v_r which may be as low as 0.8 km/s, representative of the surface temperature at 150 km. A typical freestream velocity V_s is about 8 km/s, so the freestream density n_0 builds up to $n \cong n_0 V_s/v_r \simeq 10 n_0$ in front of the surface as the flux of molecules emitted equilibrates with the incident flux intercepted by the surface. Under the rough assumption that the molecule-molecule collision cross section is constant in the velocity range from v_r to V_s, the mean free path in front of the surface is reduced to $\lambda = \lambda_0 v_r/V_s \simeq 0.1\lambda_0$. Hence, significant energy accommodation may lead to a reduction in Knudsen number from about 40 to 4. At these low values, about 20% of the molecules reflected in the forward direction from the center of the disk of diameter D will undergo their "first collision" within $1D$ unit ($D \simeq 1$ m, in the case discussed here), producing a significant deviation from free-molecular flow. The actual fraction of all molecules undergoing "first collision" within $1D$ is somewhat smaller than 20% because of the finite diameter and the decrease of n with distance from the center of the disk. It is assumed herein that the effective Knudsen number is always sufficiently large that "first collision" deviations from free-molecular flow can be neglected.

The cylindrical spacecraft of the proposed NASA Geopotential Research Mission (GRM) are to be flown with attitude control to maintain zero angle of attack for minimal drag, and fueled to keep constant altitude in circular orbits at 160 km for extended periods of time.[2,3] That project has brought attention to the drag problem and to the prediction of drag coefficients for long cylindrical spacecraft in which the length is greater than several times the diameter. Most spacecraft for which drag has been measured reliably in flight were spheres, or short cylinders (diameter $\simeq$ length), and the large body of data available on these spacecraft has shown that prediction of the drag coefficient is good. However, for long cylinders the data base is small, and the drag measurements are often complicated by the uncertain state of the attitude in flight. Nonetheless, there are some measurements available that were carried out with attitude control, and these can be used in conjunction with the results presented here to predict drag coefficients for other cylindrical spacecraft.

The approach taken in this paper is based on the realistic notion that the drag force on the side of the cylinder is due to molecular rays impacting the surface at some average angle of incidence $\langle\theta_i\rangle$, less than 90 deg. This impact angle is given roughly by the ratio V/a, where V is the spacecraft velocity and $a=(2kT/m)^{1/2}$ the most probable speed of a gas at temperature T and molecular mass m. k is the Boltzmann constant. The angle $\langle\theta_i\rangle$ corresponds to the direction of the net incident momentum vector, and this is known precisely. The fractional momentum imparted to the surface along the line of incidence[4] is used to compute the drag force instead of using the normal and tangential accommodation coefficients.[5] This approach gives a lateral surface drag coefficient for the cylinder in terms of two microscopic quantities: $\langle\theta_i\rangle$ and the fractional momentum value corresponding to $\langle\theta_i\rangle$. In addition, the method gives expressions for the drag coefficient of several common shapes that may be evaluated readily using laboratory data.

Previous calculations of the lateral surface drag coefficient of the cylinder were reported by Sentman[6] and Moe and Tsang.[7] Sentman assumed that the molecules were re-emitted diffusively after impact, and Moe and Tsang derived an ex-

Received Dec. 12, 1983; revision submitted July 20, 1984. This paper is declared a work of the U.S. Government and therefore is in the public domain.

*Space Scientist, Laboratory for Planetary Atmospheres.

pression for the coefficient in terms of Schamberg's analytic representation of the molecule-surface interaction.[8] Experimental results obtained subsequent to Sentman's report showed that diffuse re-emission dominates only at low impact velocities. At typical orbital velocities (8 km/s), specular reflection is at least as strong as diffuse,[9,10] and must be accounted for in a realistic calculation. Specular reflection was included by Moe and Tsang implicitly through Schamberg's model. However, they ignored the effect of thermal motion, and their expression requires the ratio of the re-emitted to the incident velocities at a 90-deg impact angle for the lateral surface of the cylinder. Additional parameters specified in Schamberg's model must be used in their expression, and the velocity ratio and the other parameters are not accessible readily. Nonetheless, it is shown below that when reasonable values of those parameters are used in their expression, the numbers compare favorably with the results in this work.

The principal advantages of the approach presented here are: 1) the effect of thermal motion in the atmosphere is included explicitly, 2) a simple expression for the drag coefficient is obtained which can be used to estimate the lateral surface drag from flight drag data, and 3) the lateral surface drag coefficient is expressed in terms of two microscopic parameters, one of which is accessible from general kinetic theory and the other from laboratory data.

The next section discusses the effect of thermal motion on self shadowing and its influence on the value of the impact angle $\langle\theta_i\rangle$. The third section contains the derivations of the drag force and the lateral surface coefficient. The fourth section uses previous flight data to estimate the lateral surface coefficient for an aluminum surface, and compares that number with the number obtained using the microscopic parameters. The last section discusses the significance of the lateral surface coefficient in the light of previous results and its application to future spacecraft such as the NASA GRM.

Kinetic Theory

Consider a surface element moving with velocity $\vec{V}$ in a uniform rarefied gas with number density n_0. The surface normal $\hat{n}$ is tilted at the surface angle θ to $\vec{V}$. If the gas is at rest, the line of impact of individual molecules is determined by the sum $-\vec{V}+\vec{v}$, where $\vec{v}$ is the random molecular velocity. In the coordinate frame of the moving surface, the gas moves toward the surface with bulk velocity $\vec{V}$, as shown in Fig. 1, and the molecular velocities are distributed according to the drifting Maxwellian distribution

$$f_M(\vec{v}) = n_0\left(\frac{1}{\pi a^2}\right)^{3/2}\exp[-((v_x-V)^2+v_y^2+v_z^2)/a^2] \quad (1)$$

where v_x, v_y, and v_z are the velocity components along the corresponding axes. In Fig. 1 the y axis points out of the plane of the paper.

When $\theta=0$, the numbers of impacting molecules with negative and positive v_z components are equal, and the average impact velocity is exactly equal to $\vec{V}$. However, as soon as θ departs from zero, the perfect cancellation of the thermal motion in the z axis ceases, and the impact velocity differs from $\vec{V}$. For example, if $\theta>0$, some molecules with $v_z<0$ are masked by the back of the surface. Hence, more molecules with $v_z>0$ than $v_z<0$ impact the surface. This self shadowing gives rise to a nonzero average component in the z direction whose magnitude increases with θ. This means that the average incident momentum vector departs from the line of impact by an amount that increases with θ. A measure of this departure may be taken then as a measure of self shadowing.

The direction of incident momentum can be obtained from previous results,[5] giving the pressure P_i and shear τ_i due to the incident molecules alone. As they have shown,[5] these quantities may be obtained from the average forces integrated over the distribution function $f_M(\vec{v})$. The resulting expressions are

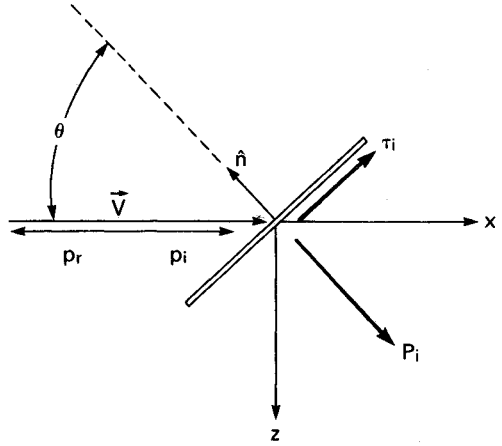

Fig. 1 Side view of surface element impacted by a beam with velocity $\vec{V}$. The incident momentum density $\vec{p}_i$ is equal to $\rho\vec{V}$, ρ being the mass density in the beam. p_r is the re-emitted momentum component along the line of $\vec{p}_i$. Also shown are the pressure P_i and shear stress τ_i due to the incident beam.

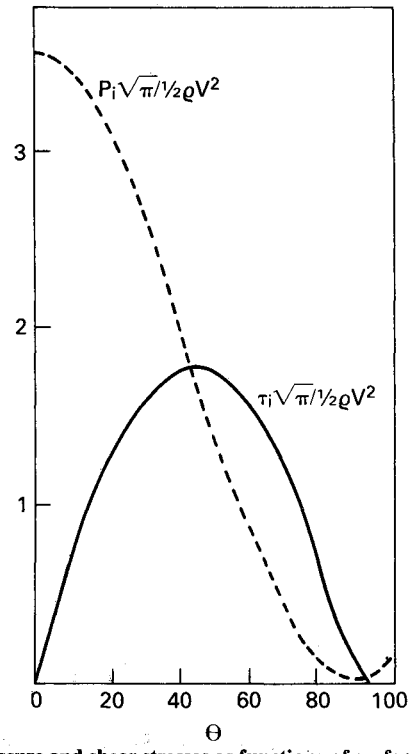

Fig. 2 Pressure and shear stresses as functions of surface angle θ for $s=10$. Both quantities are given in units of $\frac{1}{2}\rho V^2/\sqrt{\pi}$ for convenience.

$$P_i(s,\theta) = \frac{\rho V^2}{2(\pi)^{1/2}}\frac{1}{s^2}\{te^{-t^2}+\sqrt{\pi}(\tfrac{1}{2}+t^2)(1+\mathrm{erf}(t))\} \quad (2)$$

and

$$\tau_i(s,\theta) = \frac{\rho V^2}{2(\pi)^{1/2}}\frac{\sin\theta}{s}\{e^{-t^2}+\sqrt{\pi}t(1+\mathrm{erf}(t))\} \quad (3)$$

where θ is the surface angle as defined above, $s=V/a$, and $t=s\cos\theta$.

Figure 2 shows the variation of P_i and τ_i with θ for $s=10$. This value of s corresponds to an orbital velocity of about 8 km/s and a molecular nitrogen atmosphere at a temperature of 1000 K. If multiplied by the area of the surface, P_i and τ_i

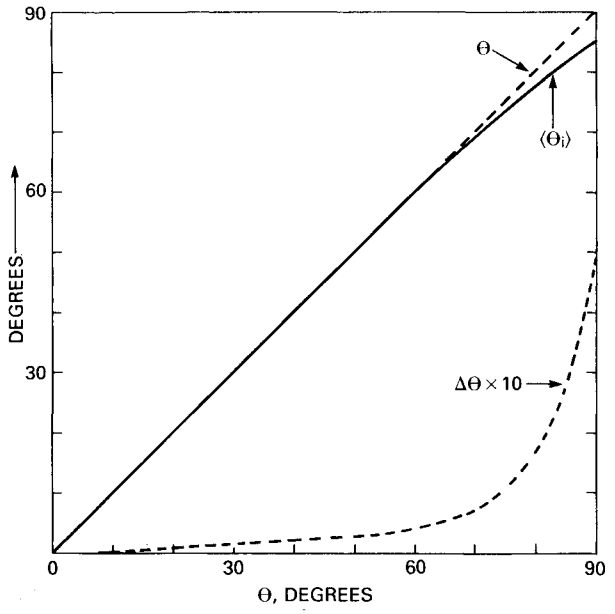

Fig. 3 Variation of impact angle $\langle\theta_i\rangle$ with surface angle θ. $\Delta\theta=\theta-\langle\theta_i\rangle$ is magnified 10 times to show region where self shadowing becomes significant.

give the normal and tangential components of the force exerted on the surface if all of the incident momentum is absorbed. These two quantities are, in fact, the normal and tangential momentum flux components. Therefore, the average impact angle of the net momentum vector is given by

$$\langle\theta_i\rangle=\tan^{-1}(\tau_i/P_i) \tag{4}$$

The departure of $\langle\theta_i\rangle$ from the surface angle θ is plotted in Fig. 3. θ and $\langle\theta_i\rangle$ are plotted against θ, and the difference $\Delta\theta=\theta-\langle\theta_i\rangle$, magnified 10 times, is shown. For values of θ greater than 86 deg, the departure exceeds about 5% of θ, and may not be ignored in careful computations of the drag force. Self shadowing becomes increasingly important as the surface angle varies from roughly 85 to 90 deg. Figure 3 also shows that the impact angle $\langle\theta_i\rangle$ is about 85 deg at $\theta=90$ deg for $s=10$. The near coincidence of these two angles is not fortuitous; see further discussion below.

In the following sections the drag coefficient is obtained with due consideration to the value of $\langle\theta_i\rangle$. For a different value of s, $\langle\theta_i\rangle$ may be obtained from Eq. (4), evaluated at $\theta=90$ deg.

The Drag Force on a Cylindrical Spacecraft

The drag force $\vec{F}_D$ on a cylindrical spacecraft flying at zero angle of attack in a rarefied atmosphere at high Knudsen number may be written as

$$\vec{F}_D=\vec{F}_f+\vec{F}_{LS} \tag{5}$$

where $\vec{F}_f$ is the drag force on the front face which is typically a flat plate or nose cone, and $\vec{F}_{LS}$ the drag force resulting from grazing molecular impacts on the lateral surface of the cylinder. By definition, these two vectors are antiparallel to the direction of flight. The condition of high Knudsen number guarantees that no forces are exerted on surfaces masked by the front and sides.

Force on the Front Face

The magnitude of the term $\vec{F}_f$ is obtained from the drag coefficient C_{Df} corresponding to the shape of the front face using

$$\vec{F}_f=\tfrac{1}{2}C_{Df}\rho V^2A_n \tag{6}$$

where ρ is the local mass density of the atmosphere, V the magnitude of the spacecraft velocity relative to the atmosphere, and A_n the projection of the front face surface area along the direction of flight.[5] In the case presented herein $A_n=\pi r^2$, where r is the radius of the projected disk, which is also the radius of the base of the cylinder.

An explicit form for C_{Df} can be obtained at this point using an approach based on the laboratory measurements of Boring and Humphris.[4] They measured the fraction of momentum reflected or re-emitted in the direction of the incident momentum vector for several angles of incidence from 0 to 75 deg. That fraction is designated as

$$f(\theta_i)=p_r/p_i$$

where θ_i is the impact angle of Eq. (4) between vector $\vec{p}_i$ and the surface normal $\hat{n}$, and p_r the component of the reflected or re-emitted momentum along the line parallel to $\vec{p}_i$. The values of $f(\theta_i)$ to be used below will be obtained from experimental data. The net momentum delivered to the surface along this direction is p_i+p_r. In the absence of bulk velocities in the atmosphere (e.g., winds), this is the component along the direction of flight responsible for the drag. For most front faces $\theta_i<85$ deg, so in this case $\theta_i=\theta$. Figure 1 shows $\vec{p}_i$ and p_r acting on an element of surface dA. The elemental drag force on dA is given by the momentum flux intercepted by the projection of dA along $\vec{V}$ multiplied by the net fraction of momentum delivered to the surface. That is,

$$dF_D=(1+f(\theta))\rho V^2\cos\theta dA \tag{7}$$

The drag force on a body defined by an impact surface Σ is then obtained by integrating Eq. (7) over such a surface:

$$F_D=\int_\Sigma (1+f(\theta))\rho V^2\cos\theta dA \tag{8}$$

For the case of Knudsen numbers considered herein, the impact surface Σ is made up of those elements of the body surface whose normals have nonzero positive components in the direction of flight that are larger than some minimum value $\cos\theta_m$. The angle θ_m is the angle beyond which self shadowing of the surface becomes significant. As shown above $\theta_m\simeq 85$ deg.

Equation (8) can be generalized to apply to shapes in which θ exceeds θ_m, such as spheres, ellipsoids, sharp cones, etc. That generalization requires the definition of an effective density term $\rho_{eff}(\theta)$ to be used in place of the constant density ρ in Eq. (8). Note also that the term V would be replaced by a net incident velocity term which would also depend on θ. The function $\rho_{eff}(\theta)$ would perhaps provide a more meaningful measurement of self shadowing, but this more general treatment is not necessary for the purposes stated herein.

Equation (8) is now used to obtain the drag coefficient for three common shapes: a flat plate, a full cone, and a truncated cone. Each case is illustrated in Fig. 4.

For a flat plate with normal $\vec{n}$ inclined at an angle θ to $\vec{V}$, the drag coefficient obtained usings Eqs. (6) and (8) is

$$C_{D(\text{flat plate})}=2[1+f(\theta)] \quad \text{for} \quad \theta\lesssim 85 \text{ deg} \tag{9}$$

For a cone with half-angle ϕ flying with its axis parallel to $\vec{V}$, the drag coefficient is, by Eqs. (6) and (8),

$$C_{D(\text{cone})}=2\left[1+f\left(\frac{\pi}{2}-\phi\right)\right] \quad \text{for} \quad \phi\gtrsim 5 \text{ deg} \tag{10}$$

Similarly, the drag coefficient for a cone with base radius a truncated at the top by a flat circular plate with radius b is

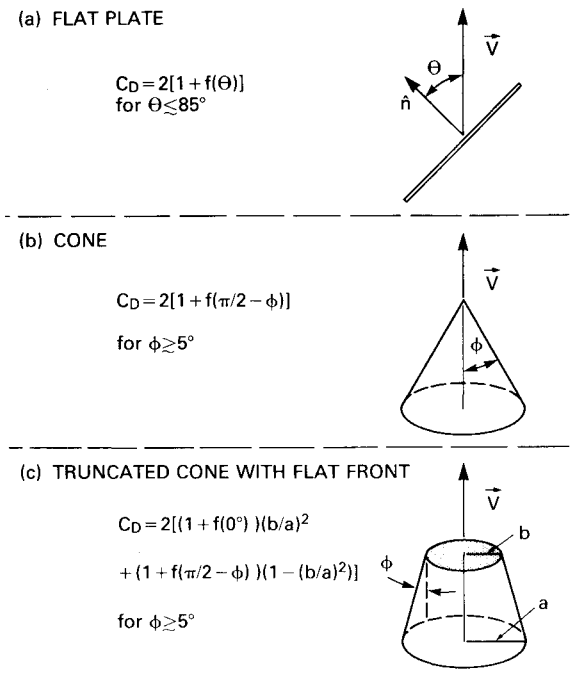

Fig. 4 Drag coefficients for simple shapes.

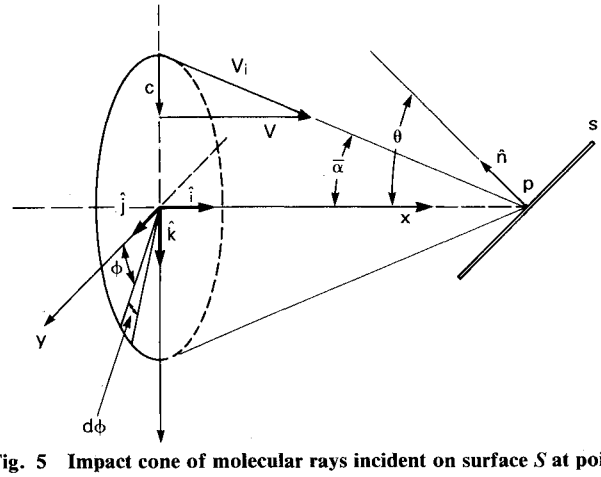

Fig. 5 Impact cone of molecular rays incident on surface S at point P.

given by

$$C_{D(\text{truncated cone with flat top})} = 2\left[(1 + f(0 \text{ deg}))\frac{b^2}{a^2} + \left(1 + f\left(\frac{\pi}{2} - \phi\right)\right)\left(1 - \frac{b^2}{a^2}\right)\right] \tag{11}$$

where $\phi \geq 5$ deg.

Equations (9-11) show that the function $f(\theta)$ of Boring and Humphris[4] provides a convenient way to represent the drag coefficient directly in terms of laboratory results. The last expression is used below in conjunction with their experimental data.

Drag Force on the Lateral Surface

The relation between self shadowing and the impact angle $\langle\theta_i\rangle$ will be discussed now, taking thermal motion into account; that is, for the following, $\theta_i \neq \theta$, their difference being as given in Fig. 3. At the end of this section the expression for the drag force on the lateral surface is obtained.

First, let us assume that the molecules imparting momemtum at point P in Fig. 5 move on the average along rays making an angle $\bar{\alpha}$ with the x axis. These rays describe a cone of half angle $\bar{\alpha}$ as shown in Fig. 5. This is a valid description since the velocity distribution of the gas molecules in the plane perpendicular to $\vec{V}$ is that of a two-dimensional Maxwellian gas at rest. The angle $\bar{\alpha}$ is determined by the average velocity c in all radial directions of the y-z plane; shown in the Appendix to be $c = \sqrt{\pi a}/2$. Thus, the cone half-angle is $\bar{\alpha} = \tan^{-1}(\sqrt{\pi a}/2V)$.

Inspection of Fig. 5 shows that as θ increases the rays begin to be intercepted by the surface at an angle $\theta_m = \pi/2 - \bar{\alpha}$. Thus, self shadowing occurs when $\theta \geq \theta_m$. Of course, it is clear that self shadowing begins gradually before θ reaches θ_m because of the smooth distribution in velocities, as shown in Fig. 3.

The case $\theta = \pi/2$ corresponds to the lateral surface of the cylinder of the spacecraft. Reference to Fig. 5 shows that only half of the molecular rays would reach point P for this angle. Therefore, the thermal motion gives a nonzero component in the plane perpendicular to the surface which contains $\vec{V}$ represented by a beam of density $\rho/2$ and incident velocity $\vec{V}_i$ upon the surface. $\vec{V}_i$ is given by

$$\vec{V}_i = \hat{i}V + \hat{k}c \tag{12}$$

where the unit vectors are illustrated in Fig. 4. It is shown in the Appendix that the direction of $\vec{V}_i$ in this treatment is exactly equal to $\langle\theta_i\rangle$ obtained from Eq. (4) for $\theta = \pi/2$. The elemental force on area dA is

$$d\vec{F} = \tfrac{1}{2}\rho \vec{V}_i V_i (1 + f(\theta_i))\cos\theta_i dA \tag{13}$$

where $\theta_i = \bar{\alpha}$, the angle of incidence of the vector of Eq. (12).

The momentum $\vec{p}_{r\perp}$ reflected perpendicular to $\vec{p}_i$ will have a component along the surface which contributes to the drag force. However, for angles $\theta_i \gtrsim 85$ deg, this contribution is small in comparison to the contribution due to p_r, therefore, it is ignored. The validity of this assumption rests on 1) the component of $p_{r\perp}$ that contributes to drag is proportional to $\cos\theta_i < 0.07$, and 2) the function $f(\theta)$ has an absolute value approaching 1 at $\theta \gtrsim 85$ deg (see Ref. 4). This is equivalent to the findings of Saltsburg and Smith[9] and Hays et al.,[10] that the surface scattering is strongly specular at high impact velocities. Now, the energetics require that $(f(\theta))^2 \leq 1$. Therefore, at these angles, the ratio $p_{r\perp}/p_i$ approaches zero as $f(\theta)$ approaches unity.

Integration of the vector $d\vec{F}$ over the entire lateral surface gives the term $\vec{F}_{LS}$. Its magnitude is

$$F_{LS} = \tfrac{1}{2}\rho V_i^2 A_{LS} \sin\theta_i \cos\theta_i [1 + f(\theta_i)] \tag{14}$$

where $A_{LS} = \pi r L$ = lateral surface area of cylinder of radius r and length L.

Substituting Eqs. (6) and (14) into Eq. (5), eliminating V_i, and dividing by the factor $\tfrac{1}{2}\rho V^2 A_n$, the drag coefficient for the cylindrical spacecraft is obtained. That is,

$$C_D = C_{Df} + (2L/r)C_{LS} \tag{15}$$

where

$$C_{LS} = \cot\theta_i [1 + f(\theta_i)] \tag{16}$$

Equation (15) is the desired scaling law for a cylindrical spacecraft flying parallel to its principal axis. It is used below with flight data to obtain C_{LS}. Intuitively it is known that the drag due to the lateral surface must be directly proportional to the length of the cylinder. Equation (15) tells us that the length of the cylinder is to be specified in units of the radius of the cylinder, since the radius is the basic parameter for the frontal area. Note that the ratio of lateral area to frontal area is precisely $2L/r$, the factor that multiplies C_{LS}.

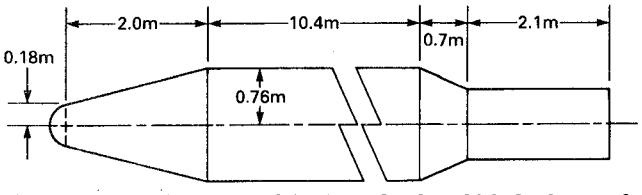

Fig. 6 Critical dimensions of Agena rocket for which the drag coefficient was measured at zero angle of attack.

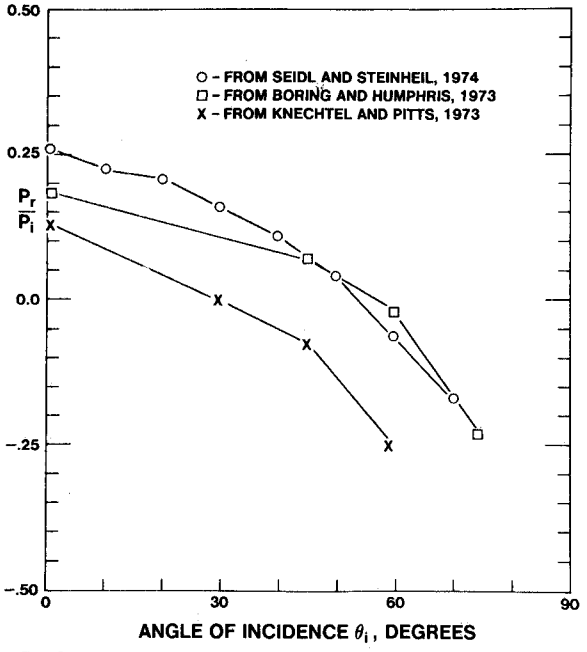

Fig. 7 Comparison of the ratio p_r/p_i obtained from the three experiments referenced.

Estimates of C_{LS}

The drag coefficient has been measured for a cylindrical spacecraft flying at zero angle of attack, and the drag computations have been reported by Robertson.[11] The spacecraft used was an Agena rocket with dimensions as given in Fig. 6. The drag coefficient obtained by Robertson from the flight data was $C_D = 3.3$.

An estimate for C_{LS} can be obtained using the data for the Agena rocket in conjunction with the laboratory measurements of Boring and Humphris.[4] The latter is used to obtain C_{Df} for the nose cone with Eq. (11), and Eq. (15) with the known L/r ratio to obtain C_{LS}.

From Fig. 6, the half-angle of the truncated nose cone is $\phi \simeq 11$ deg. As shown below, the data of Boring and Humphris[4] extrapolate to a value $f[(\pi/2)-\phi] = f(79 \text{ deg}) = -0.40$. Therefore, using Eq. (11) with $b = 36$ cm and $a = 76$ cm, the drag coefficient of the nose cone is $C_{Df} = 1.5$. From Fig. 6, $2L/r \simeq 30$. Substituting this and $C_D = 3.3$ into Eq. (15) gives $C_{LS} = 0.06$ for the buffed aluminum surface of the Agena rocket.

Figure 7 is taken from a recent review of momentum accommodation coefficient measurements.[12] It compares the direct measurements of $f(\theta)$ by Boring and Humphris (squares), with $f(\theta)$ obtained from the momentum accommodation coefficients measured by Seidl and Steinheil[13] (circles) and Knechtel and Pitts[14] (×). The data sets of both Knechtel and Pitts (KP) and Boring and Humphris (BH) correspond to N_2 and N_2^+ molecular impact at velocities of about 8 km/s. In KP the target surface was aluminum, and in BH test surfaces from satellites Echo I and Explorer XXIV were used. The data set of Seidl and Steinheil (SS) corresponds to He atom impact on a sapphire surface at a velocity of 2 km/s. Boring and Humphris showed that $f(\theta)$ decreases with impact velocity, and the higher $f(\theta)$ values of the low velocity data (SS) in comparison with the other two are consistent with that finding. The large differences between KP and BH may be due to actual differences in surface characteristics. Nonetheless, these measurements may be used to estimate the lateral surface coefficient with Eq. (16).

The angle θ_i is about 86 deg. The values of $f(\theta)$ in Fig. 7 may be extrapolated to this angle, giving $f(86 \text{ deg}) \simeq -0.5 \pm 0.1$ using both BH and KP data points. Substituting in Eq. (16), $C_{LS} \simeq 0.05 \pm 0.01$, in close agreement with the value obtained above from the Agena rocket drag data.

This value of C_{LS} means that for a length-to-diameter ratio of 5, the drag coefficient contribution of the lateral surface is approximately 1.2, close to the contribution of the front face, $C_{Df} \simeq 1.5$.

Discussion

It is interesting to analyze the equivalent expression of C_{LS} obtained by Moe and Tsang[7] in the light of the results obtained here. Equation (2) of their paper gives

$$C_{LS} = 2(1 + (V_r/V_i)\Phi(\phi_0) f(\nu))$$

where V_r and V_i are the re-emitted and incident velocities, respectively. $\Phi(\phi_0)$ is a factor which accounts for the fact that not all of the re-emitted molecules are directed along a single line, and $f(\nu)$ depends on the angle of attack as well as the factor ν. $\Phi(\phi_0)$ and ν must be determined from Schamberg's model. Nevertheless, for zero angle of attack, Fig. 3 of Ref. 7 shows that $f(\nu) = -1$ for all ν. Setting $C_{LS} = 0.05$ gives

$$(V_r/V_i)\Phi(\phi_0) \simeq 0.97$$

Assuming that $\Phi(\phi_0) \simeq 1$ as it should be for strong specular scattering, this result is consistent with the finding that $V_r/V_i \to 1$ at $\theta \to 90$ deg.

The results obtained here can be applied to spacecraft which feature attitude control to maintain zero angle of attack, like those proposed for the NASA GRM. With this feature, the shape of the spacecraft can be optimized to reduce the drag significantly. The discussion on self shadowing and Fig. 2 suggest that lateral surface drag may be reduced substantially by adjusting θ_i to the neighborhood of 90 deg. This is obtained with an almost-cylindrical spacecraft in the shape of a truncated cone with a small half-angle of a few degrees. The exact value of the half-angle would be determined by the desired drag reduction and the atmospheric temperature expected during flight.

Appendix

The average velocity c used in the discussion preceding Eq. (12) is the average of all molecules incident upon point P in Fig. 5 from the azimuthal range $(\phi, \phi + d\phi)$. Since the distribution is symmetric about the origin, $dv_y dv_z = v d\phi dv$.[15] Hence,

$$c = d\phi \int_0^\infty v e^{-v^2/a^2} v dv \Big/ d\phi \int_0^\infty e^{-v^2/a^2} v dv = \frac{\sqrt{\pi} a}{2}$$

where $v^2 = v_y^2 + v_z^2$.

In the case of interest, $\theta = \pi/2$ and the value c represents the average velocity perpendicular to the surface. The velocity parallel to the surface is just the velocity V of Eq. (12).

Now, in order to compute the pressure and shear forces the mass flux incident on the surface when $\theta = \pi/2$ must be known (see Fig. 5). This is given by

$$\vec{J} = \int_0^{-\infty} \int_{-\infty}^{\infty} \int_{-\infty}^{\infty} m f_M(\vec{v}) (\hat{i} v_x + \hat{j} v_y + \hat{k} v_z) dv_x dv_y dv_z$$

where $f_M(\vec{v})$ is given in Eq. (1) and m is the molecular mass.

The above integral gives

$$\vec{J}=\frac{mn_0}{2}[\hat{i}V+\hat{k}\bar{v}]$$

where $\bar{v}=a/\sqrt{\pi}$.

In this expression, the z component $\hat{k}\bar{v}$ is responsible for transporting the momentum to the surface. Thus, the pressure, being the flux of normal momentum, is

$$P=\bar{v}c=(n_0m/4)a^2$$

Similarly, the shear, being the flux of transverse momentum mV transported to the surface at rate $n_0\bar{v}/2$, is

$$\tau=\frac{n_0m}{2}V\bar{v}=\frac{n_0m}{2\sqrt{\pi}}Va$$

These values of P and τ are identical to those obtained from Eqs. (2) and (3) for $\theta=\pi/2$, showing that the vector of Eq. (12) does correspond to the incident momentum vector.

The ratio τ/P gives the impact angle θ_i of Eq. (13). From the two equations above,

$$\theta_i=\tan^{-1}\left(\frac{V}{c}\right)=\tan^{-1}\left(\frac{2V}{\sqrt{\pi}a}\right)$$

This is precisely the angle $\langle\theta_i\rangle$ obtained with Eq. (4) setting θ to $\pi/2$ in τ_i and P_i.

References

[1]Cook, G. E., "Satellite Drag Coefficients," *Planetary Space Science*, Vol. 13, Oct. 1965, pp. 929-946.

[2]Keating, T., "Geopotential Research Mission (GRM)," AIAA Paper 83-0347, Aug. 1983.

[3]Ray, J. C. and Jenkins, R. E., "GRAVSAT/MAGSAT—A Guidance and Control System," The Johns Hopkins University, Applied Physics Laboratory, Columbia, Md., Annual Report 1981, Vol. 1, JHU/APL SDO 6179, 1981.

[4]Boring, J. W. and Humphris, R. R., "Drag Coefficients for Free Molecule Flow in the Velocity Range 7-37 km/s," *AIAA Journal*, Vol. 8, 1970, pp. 1658-1662.

[5]Schaaf, S. A. and Chambre, P. L., "Flow of Rarefied Gases," *Fundamentals of Gas Dynamics*, edited by H. W. Emmons, Princeton University Press, Princeton, N.J., 1958, pp. 692-705.

[6]Sentman, L. H., "Free Molecule Flow Theory and its Application to the Determination of Aerodynamic Forces," Lockheed Missiles and Space Co., Sunnyvale, Calif., LMSC-448514, Oct. 1961.

[7]Moe, M. M. and Tsang, L. C., "Drag Coefficients for Cones and Cylinders According to Schamberg's Model," *AIAA Journal*, Vol. 11, March 1973, pp. 396-399.

[8]Schamberg, R., "A New Analytic Representation of Surface Interaction for Hyperthermal Free Molecule Flow," The Rand Corp., Santa Monica, Calif., RM-2313, Jan. 1959.

[9]Saltsburg, H. and Smith Jr., J. N., "Molecular Beam Scattering from the (111) Plane of Silver," *Journal of Chemical Physics*, Vol. 45, 1966, pp. 2175-2183.

[10]Hays, W. J., Rodgers, W. E., and Knuth, E. L., "Scattering of Argon Beams with Incident Energies up to 20 eV from a (111) Silver Surface," *Journal of Chemical Physics*, Vol. 56, Feb. 1972, pp. 1652-1657.

[11]Robertson, A., "Comparison of Flight-Measured Drag Characteristics with Pre-flight Predictions," Aerospace Corp., El Segundo, Calif., Internal Rept. 71-5131.1-34, July 1971.

[12]Herrero, F. A., "The Drag Coefficient of Cylindrical Spacecraft in Orbit at Altitudes Greater than 150 km," NASA TM-85043, May 1983.

[13]Seidl, M. and Steinheil, E., "Measurement of Momentum Accommodation Coefficients on Surfaces Characterized by Auger Spectroscopy, SIMS and LEED," *Rarefied Gas Dynamics, Proceedings of 9th International Symposium 1974*, Vol. II, edited by M. Becker and M. Fiebig, DFVLR Press, Germany, 1974, pp. E.9-1—E.9-12.

[14]Knechtel, E. D. and Pitts, W. C., "Normal and Tangential Momentum Accommodation for Earth Satellite Conditions," *Astronautica Acta*, Vol. 18, June 1973, pp. 171-184.

[15]Loeb, L., *The Kinetic Theory of Gases*, Dover Publications, New York, 1961, pp. 278-348.